



Cu–water nanofluid flow with arbitrarily shaped nanoparticles over a porous plate in a porous medium in the presence of slip

SWATI MUKHOPADHYAY¹ *, MANI SHANKAR MANDAL² and K VAJRAVELU³

¹Department of Mathematics, The University of Burdwan, Burdwan 713 104, India

²Department of Mathematics, Govt. General Degree College, Kalna-I, Burdwan 713 405, India

³Department of Mathematics, University of Central Florida, Orlando, FL 32816-1364, USA

*Corresponding author. E-mail: swati_bumath@yahoo.co.in

MS received 25 February 2022; revised 30 May 2022; accepted 10 June 2022

Abstract. The objective of the article is to analyse the forced convection nanofluid flow over a permeable plate in an absorbent medium using slip boundary conditions. A single-phase model for the nanofluid is used with variable shapes of nanoparticles. The partial differential equations (PDEs) of the model are altered into a set of non-linear ordinary differential equations (ODEs) by a suitable alteration. To obtain the solutions of the system of equations numerically, Runge–Kutta method is used with a shooting technique. The effects of various parameters, like permeability, suction/injection, nanoparticle volume fraction, velocity slip, thermal slip and nanoparticle shape parameters on velocity and temperature profiles are presented graphically and analysed. In addition, for a clear understanding of the model, the flow and the heat transfer characteristics are presented through graphs and analysed. Fluid velocity is found to increase with the increasing values of permeability of the porous medium, whereas temperature is found to reduce in this case. Temperature is a rising function of the thermal slip parameter, whereas it is a decreasing function of the velocity slip parameter.

Keywords. Nanofluid; forced convection; porous medium; arbitrarily shaped nanoparticles; partial slips; permeable plate.

PACS Nos 44.20.+b; 44.27.+g; 44.30.+v

1. Introduction

Nanotechnology has attracted enormous attention among researchers due to its widespread applications in manufacturing processes and medical sciences. Nanofluid is an innovative class of fluids, the concept for which has been planned as a foundation for increased performance of heat transport fluids. To augment the thermal conductivity of the base fluid (viz., water, ethylene glycol, oil), which has low thermal conductivity, nanometre-sized elements are scattered in the base liquid. To permit more heat transfer, usually, these elements are prepared of metal or metal oxide to supplement the conduction and convection coefficients. Choi [1] was the first to understand that the accumulation of nanoparticles in the base liquid tremendously augments the thermal conductivity of the liquid. Buongiorno [2] first studied the convective heat transfer in nanofluids by observing the augmentation in thermal conductivity owing to Brownian movement and thermophoretic dispersion of

nanoparticles. Later, Tiwari and Das [3] initiated a novel replica that is well accepted nowadays. Mustafa *et al* [4], Nadeem *et al* [5,6], Hussain *et al* [7], Das *et al* [8], Mabood *et al* [9], Hayat *et al* [10] and many others have investigated various aspects of nanofluid flow and heat transfer.

All these researchers considered no-slip conditions at the boundary. However, the no-slip condition at the boundary is unsuitable in situations where the exterior is sufficiently glossy. Partial slip speed is usually present at the border for emulsions, suspensions, foams, polymer solutions etc. Slip velocity at the boundary also occurs in a variety of situations, particularly in perforated plates and nets finished by wires, greased or chemically indulged hydrophobic surfaces, rough or porous surfaces (Hafidzuddin *et al* [11]), and amazing hydrophobic nanosurfaces (Choi and Kim [12], Hafidzuddin *et al* [11]). Applications of slip at the boundary are used in simulated heart valves, compound fluid problems and fluid flow on many interfaces. Hayat *et al* [13] managed

to find an analytical solution. They found the influences of slip on the flow of a second-grade liquid over an extended surface in an absorbent medium. Heat transfer performance of a boundary layer flow over a porous moving plate was examined by Mukhopadhyay *et al* [14]. Sajid *et al* [15] gave an account of the influence of slip on the flow of Maxwell liquid past an extended sheet. Nanoparticles, being extremely tiny, can allow slip speed with the molecules of the base liquid (for details, see Hussain *et al* [7]). However, much attention has not been given to recognise the effects of slip conditions on the nanofluid flows.

The heat transfer characteristics of the flow past a flat plate embedded in a porous medium are highly crucial due to its application in a group of manufacturing and engineering regulations [16]. Improved knowledge of the flow through a porous medium can be advantageous in some areas like storage of granules, processing of metals, devices for insulation, geothermal systems and devices which switch over heat, straining procedures and catalytic reactors [17–19]. In addition, flow through the absorbent media is commonly found in chemical engineering and reservoir engineering (see Mukhopadhyay and Layek [19]). Furthermore, Darcy’s law is a pragmatic principle describing the pressure gradient, bulk viscous fluid resistance and the gravitational force for a forced convection flow in a porous medium (Mukhopadhyay *et al* [20]). Aziz *et al* [21] investigated the flow of a water-based nanofluid containing gyrotactic micro-organisms past a horizontal flat plate in a porous medium. Ramana Reddy *et al* [22] investigated the rotating flow of an MHD nanofluid past a plate in a porous medium in the presence of chemical reaction and thermal radiation. Of late, Chakraborty *et al* [23] presented the effects of thermal radiation on Ag–water nanofluid flow past a plate in a non-Darcy porous medium.

To our knowledge, the steady forced convection motion of a nanoliquid with randomly formed nanoparticles with slip conditions over an absorbent plate in a permeable medium with prescribed surface temperature has not yet been investigated. With this motivation, this paper attempted to explore steady forced convection nanofluid flow past a permeable plate of the prescribed temperature embedded in a porous medium in the presence of arbitrarily shaped nanoparticles and slips at the boundary. The main goal of this study is to inspect the flow and heat transport characteristics when there are arbitrarily shaped nanoparticles and prescribed surface temperature in a porous medium. The novelty of the current research lies here. The main contribution here is to report the velocity and heat transport characteristics of motion of a nanoliquid in the presence of slip and suction/blowing at the border embedded in a porous

medium. The fluid model of Tiwari and Das [3] has been taken in the present study. The impacts of different important parameters on the nanofluid flow with arbitrarily shaped nanoparticles are presented with tables and graphs. The main contributions of this study are highlighted in §5.

2. Problem formulation and mathematical representation

Let us think about a 2D (two-dimensional) forced convection motion of a nanoliquid over an absorbent plate in a permeable medium in the presence of slip conditions at the boundary under boundary layer approximations. Let us use water as the base fluid with arbitrarily shaped Cu-nanoparticles. Let the x -axis extends along the plate and the y -axis is normal to it (see figure 1). By considering Tiwari and Das’s [3] model, the governing equations may be printed in the customary notation [19,20] as

$$\frac{\partial u}{\partial x} + \frac{\partial v}{\partial y} = 0, \tag{1}$$

$$u \frac{\partial u}{\partial x} + v \frac{\partial u}{\partial y} = v_{nf} \frac{\partial^2 u}{\partial y^2} - \frac{v_{nf}}{k} (u - u_\infty), \tag{2}$$

$$u \frac{\partial T}{\partial x} + v \frac{\partial T}{\partial y} = \frac{\kappa_{nf}}{(\rho c_p)_{nf}} \frac{\partial^2 T}{\partial y^2}, \tag{3}$$

where u and v are respectively the components of velocity in the x and y directions, $v_{nf} = \frac{\mu_{nf}}{\rho_{nf}}$ represents the kinematic viscosity of the nanoliquid, the viscosity of the nanoliquid is μ_{nf} , ρ_{nf} denotes the density of the nanofluid, $k = k_0 x$ is the permeability of the porous medium, k_0 is a constant, T denotes the temperature, κ_{nf} represents the thermal conductivity of the nanofluid and the specific heat capacitance of the nanoliquid is denoted by $(\rho c_p)_{nf}$.

The effectual possessions of the fluid are (for details, see Das *et al* [8], Hamilton and Crosser [24])

$$\begin{aligned} \rho_{nf} &= (1 - \phi)\rho_f + \phi\rho_s, \\ \frac{\kappa_{nf}}{\kappa_f} &= \frac{(n - 1)\kappa_f + \kappa_s - (n - 1)\phi(\kappa_f - \kappa_s)}{(n - 1)\kappa_f + \kappa_s + \phi(\kappa_f - \kappa_s)}, \\ \mu_{nf} &= \frac{\mu_f}{(1 - \phi)^{2.5}}, \\ (\rho c_p)_{nf} &= (1 - \phi)(\rho c_p)_f + \phi(\rho c_p)_s, \\ (\rho\beta)_{nf} &= (1 - \phi)(\rho\beta)_f + \phi(\rho\beta)_s. \end{aligned}$$

Here, the volume fraction of the solid is ϕ , μ_f indicates the dynamic viscosity of the foundation liquid, the densities of the foundation liquid and nanoparticles are respectively ρ_f and ρ_s , κ_f and κ_s are the thermal

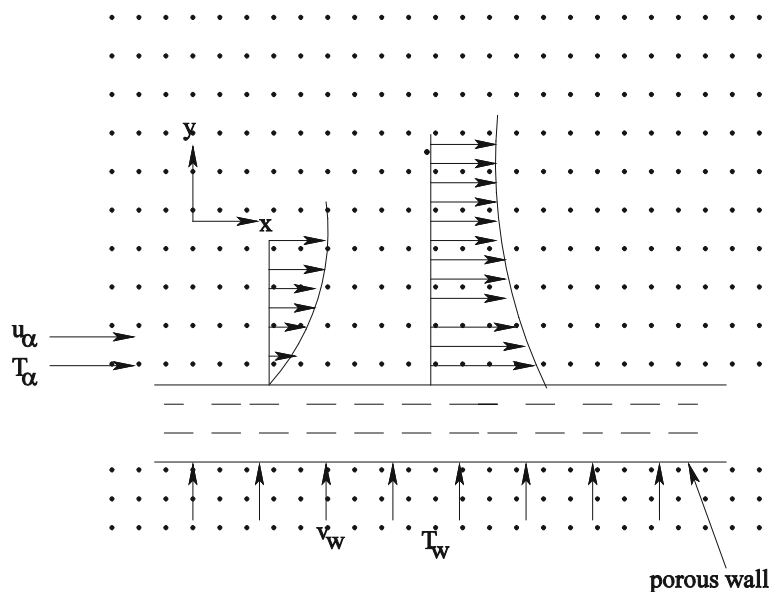


Figure 1. Sketch of the physical flow problem.

Table 1. Thermophysical properties of water, Cu and Ag (Das [25]).

	ρ (kg/m ³)	C_p (J/kg K)	κ (W/mK)	β
Cu	8933	385	401	1.67
Water	997.1	4179	0.613	21

Table 2. Values of velocity slope at the boundary $f''(0)$ for the non-absorbent plate for $k1 = 0, \phi = 0, \delta = 0$.

Blasius [26]	Howarth [27]	Cortell [28]	Ishak et al [29]	Present study
0.332	0.33206	0.33206	0.3321	0.332061

conductivities of the foundation liquid and nanoparticles, respectively. The realistic shape aspect of the nanoparticles is n , where $n = 3$ stands for the spherical nanoparticles. In this study, $n = 4.5$ has been taken to represent non-spherical nanoparticles. The thermophysical properties of water and Cu are shown (see, Das [25]) in table 1.

The boundary conditions can be expressed as

$$u = l_1 \frac{\partial u}{\partial y}, v = -v_w, T = T_w + d_1 \frac{\partial T}{\partial y} \text{ at } y = 0, \quad (4a)$$

$$u \rightarrow u_\infty, T \rightarrow T_\infty \text{ as } y \rightarrow \infty \quad (4b)$$

where

$$v_w = \frac{v_0}{\sqrt{x}}$$

is the suction ($v_0 > 0$)/injection ($v_0 < 0$) velocity,

$$T_w = T_\infty + \frac{T_0}{x}$$

is the variable temperature at the plate, T_0 is a constant. Here, the velocity slip aspect is $l_1 = l(\text{Re}_x)^{1/2}$ and the thermal slip aspect is $d_1 = d(\text{Re}_x)^{1/2}$,

$$\text{Re}_x = \frac{u_\infty x}{\nu_f}$$

is the Reynolds number, l_1, d_1 are the initial values of velocity and thermal slips.

2.1 Similarity transformation

The stream function ψ with $u = \frac{\partial \psi}{\partial y}, v = -\frac{\partial \psi}{\partial x}$ and the similarity transformation are given by

$$\begin{aligned} \psi &= \sqrt{u_\infty \nu_f x} f(\eta), \quad \eta = y \sqrt{\frac{u_\infty}{\nu_f x}}, \\ \theta &= \frac{T - T_\infty}{T_w - T_\infty}, \end{aligned} \quad (5)$$

where η is the similarity variable.

Equation (1) is automatically satisfied by ψ . With the help of (5), we get the following governing equations:

$$\begin{aligned} &\frac{1}{(1 - \phi)^{2.5} \left(1 - \phi + \phi \frac{\rho_s}{\rho_f}\right)} [f''' - k1 (f' - 1)] \\ &+ \frac{1}{2} f f'' = 0, \end{aligned} \quad (6)$$

$$\frac{\kappa_{nf} / \kappa_f}{1 - \phi + \phi \frac{(\rho c_p)_s}{(\rho c_p)_f}} \theta'' + \text{Pr} \left(\frac{1}{2} f \theta' + f' \theta \right) = 0, \quad (7)$$

where

$$\text{Pr} = \frac{\nu_f(\rho c_p)_f}{\kappa_f} \tag{8}$$

is the Prandtl number,

$$k1 = \frac{1}{Da_x \text{Re}_x} = \frac{\nu_f}{k_0 u_\infty}$$

is the permeability parameter of the absorbent medium, local Darcy number and local Reynolds' number are respectively given by

$$Da_x = \frac{k}{x^2} = \frac{k_0}{x}, \text{Re}_x = \frac{u_\infty x}{\nu_f}.$$

The boundary conditions can be written as

$$f'(0) = \delta f''(0), \quad f(0) = S, \quad \theta(0) = 1 + \beta \theta'(0), \tag{9}$$

$$f'(\eta) = 1, \quad \theta(\eta) = 0 \quad \text{as } \eta \rightarrow \infty, \tag{10}$$

where

$$S = \frac{2\nu_0}{\sqrt{u_\infty \nu_f}}$$

is the parameter responsible for suction ($S > 0$) or blowing ($S < 0$),

$$\delta = \frac{Lu_\infty}{\nu_f}$$

denotes the slip parameter corresponding to velocity whereas

$$\beta = \frac{Du_\infty}{\nu_f}$$

denotes the slip parameter corresponding to temperature.

3. Numerical method

Equations (6)–(7) are highly non-linear and exact solutions are not obtainable. So, the solutions are to be sought numerically and one must have to change the boundary value problem (BVP) shaped by (6)–(9) to an initial value problem (IVP). Using the shooting technique, the governing equations subject to the boundary conditions are solved with the help of Runge–Kutta method.

3.1 Verification of results

To confirm the validity of our results obtained numerically, assessments are completed with the available results of Blasius [26], Howarth [27], Cortell [28] and

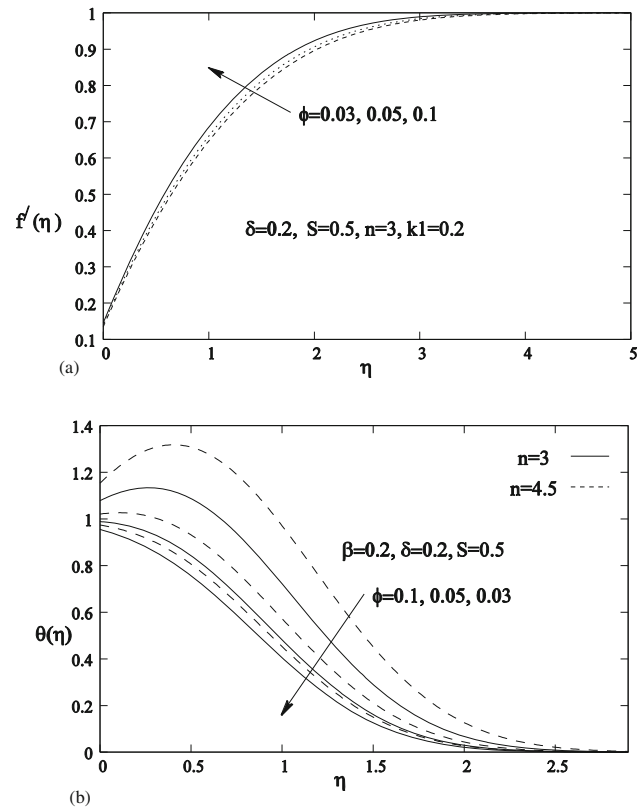


Figure 2. (a) Variation of velocity profiles with volume fraction of the nanoparticles and (b) variation of temperature profiles with volume fraction of the nanoparticles for nanoparticles of different shapes.

Ishak *et al* [29] for some specific values of the relevant parameters and excellent agreement found between the results are presented in table 2.

4. Results and discussions

Figure 2a displays the variation of velocity profiles with nanoparticle volume fraction. Fluid velocity is found to increase with a rise in the nanoparticle volume fraction ϕ . Temperature enhancement with the rise in the nanoparticle volume fraction is presented in figure 2b. Owing to an increase in nanoparticle volume fraction, an increase in thermal conductivity of the nanoliquid is observed and an increased thickness in the thermal boundary level is also found. Higher temperature is noted for higher values of the shape factor n (see figure 2b). Temperature overshoot near the plate is noticed for higher values of the nanoparticle volume fraction. Nanoparticles dissipate heat. Furthermore, heat is transferred from the fluid to the plate for higher values of volume fraction of the nanoparticles. It is a significant result and has wide applications in heat transfer phenomena. However, for lesser values of volume fraction

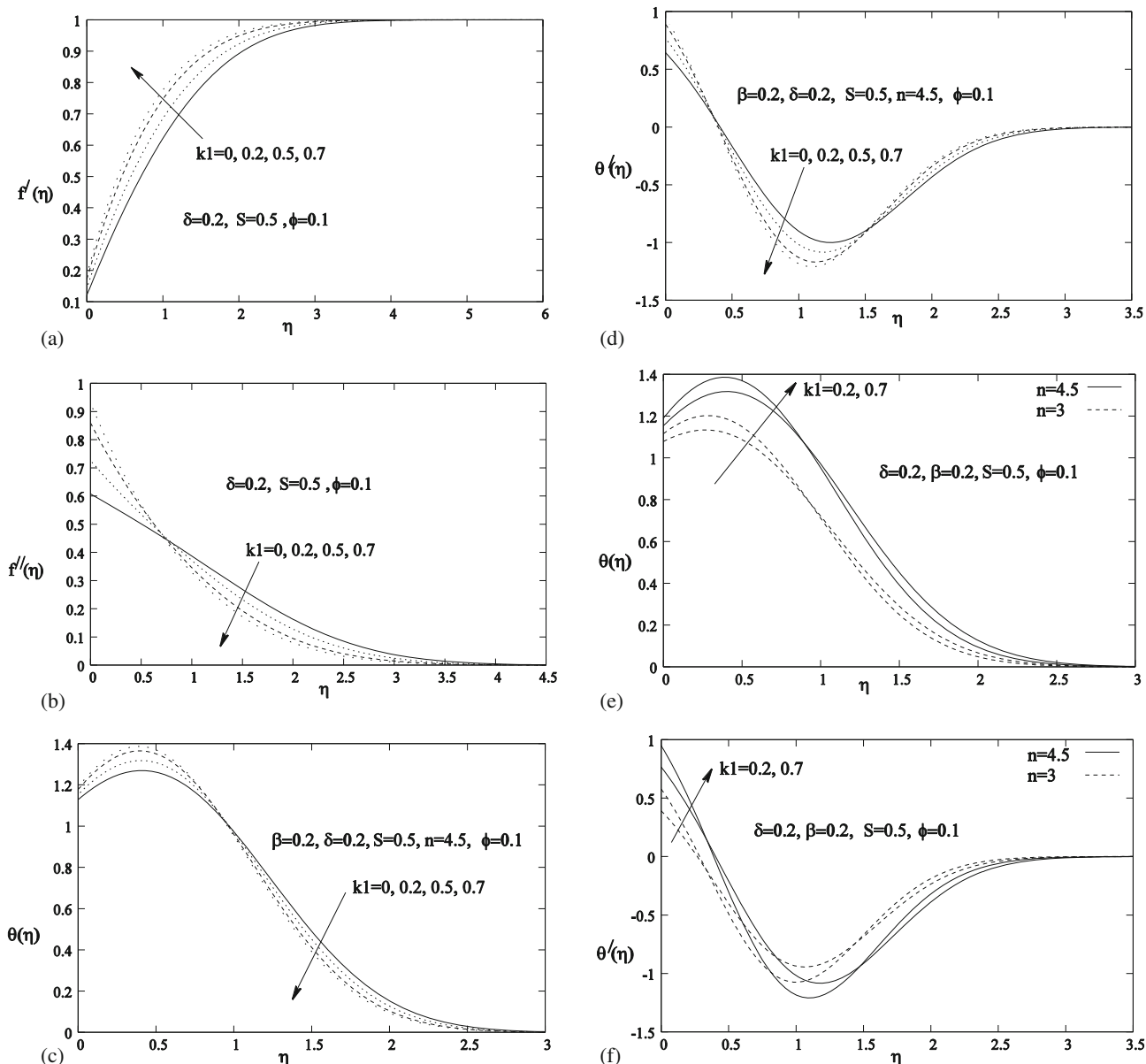


Figure 3. (a) Variation of velocity profiles for different values of k_1 of the porous medium, (b) variation of shear stress profiles for various values of k_1 of the porous medium, (c) variation of temperature profiles for different values of k_1 of the porous medium, (d) variation of temperature gradient profiles for different values of k_1 of the porous medium, (e) variation of temperature profiles with k_1 for nanoparticles of different shapes and (f) variation of temperature gradient profiles with k_1 for nanoparticles of different shapes.

of the nanoparticles, the heat is transferred to the fluid from the plate. Obviously, in the absence of nanoparticles, the base liquid (water) has the least velocity and lowest temperature.

Fluid velocity increases with a rise in the permeability parameter k_1 of the absorbent medium (figure 3a). As a result, momentum boundary layer thickness decreases with increased permeability parameter k_1 of the porous medium. Though the shear stress increases initially with a rise in the permeability parameter k_1 , finally, it

decreases (figure 3b). Due to the presence of the porous medium, fluid motion becomes restricted and the confrontation on the motion of nanofluid increases with the rise in permeability parameter of the porous medium. With an increase in permeability, the system turns out to be absorbent. As a result, the Darcian body force diminishes (since it is inversely proportional to permeability). The Darcian opposition slows down the fluid particles in continua. This confrontation reduces as the permeability of the medium increases. As a result, drag becomes

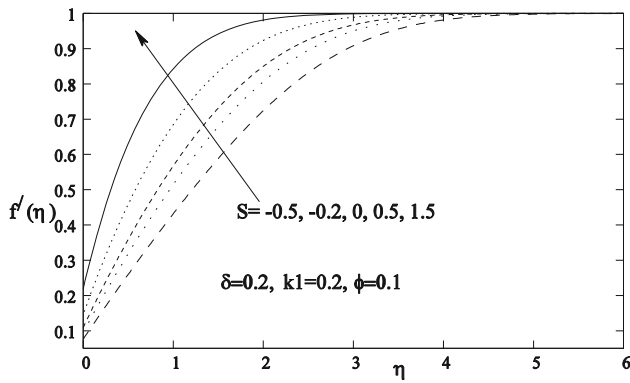


Figure 4. Velocity outlines for different values of disparity of suction/blowing parameter.

less and retardation of flow is thus reduced. Therefore, the permeability parameter improves the fluid motion within the boundary layer.

Near the plate, temperature increases with a rise in the permeability parameter k_1 but the temperature decreases. Temperature overshoot near the plate is noted (see figure 3c). The temperature gradient profile is presented in figure 3d. The thickness of the temperature boundary level reduces with the increase in the permeability parameter. Heat transport increases as the permeability parameter k_1 increases because the medium becomes absorbent in this case. Higher temperature is noted for higher values of the shape parameter n (figure 3e). Temperature overshoot is also noted near the plate (figure 3e). The temperature gradient is also higher near the plate for higher values of n (figure 3f).

The effect of suction/blowing parameter S on velocity is shown in figure 4. Fluid speed increases due to the increase in S . Consequently, the velocity boundary layer thickness decreases for augmented values of S ($S > 0$). Due to the rise in S , drag force is developed, reducing the fluid velocity. Skin friction rises in this case. However, in the case of injection ($S < 0$), the momentum boundary layer thickness increases (figure 4). Suction stabilises the motion of the fluid by controlling the boundary layer growth. It is experienced that the temperature reduces with a rise in the suction/blowing parameter S and the rate of heat transfer increases with rising values of S ($S > 0$) as the surface evaporates everywhere due to transpiration.

Figure 5a displays the behaviour of the velocity slip parameter δ on the fluid velocity. Fluid velocity increases with a rise in the velocity slip parameter, reducing the momentum boundary layer thickness (figure 5a). In the presence of slip, fluid gets a velocity at the boundary, which helps to increase the velocity within the boundary layer region. Basically, with the rise in velocity slip parameter, slip velocity

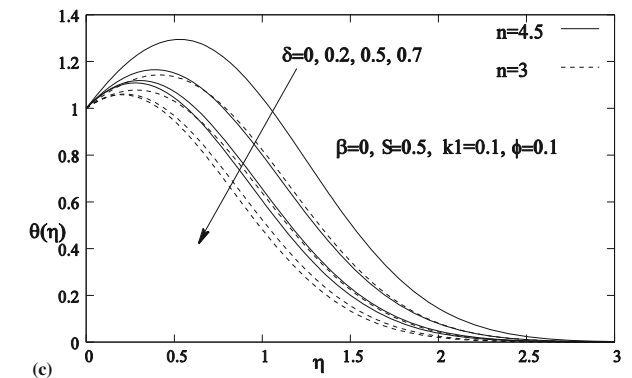
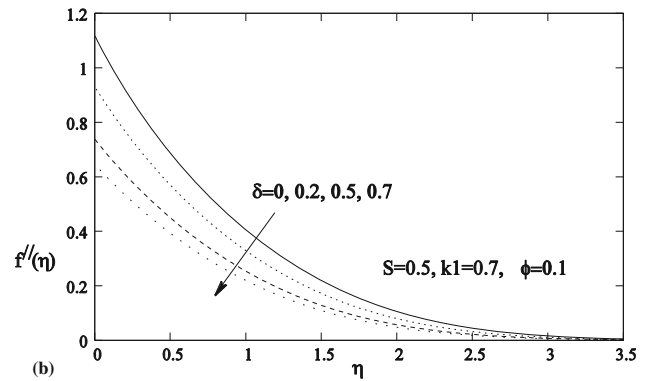
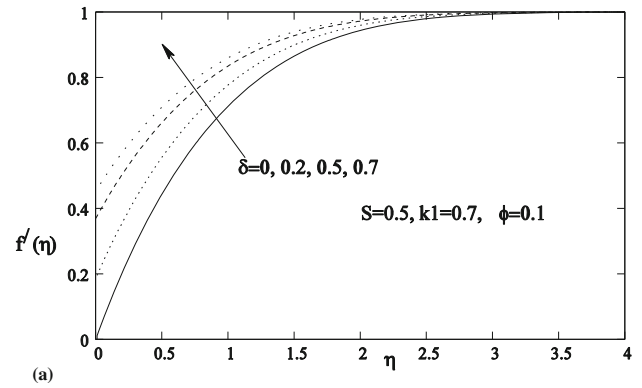
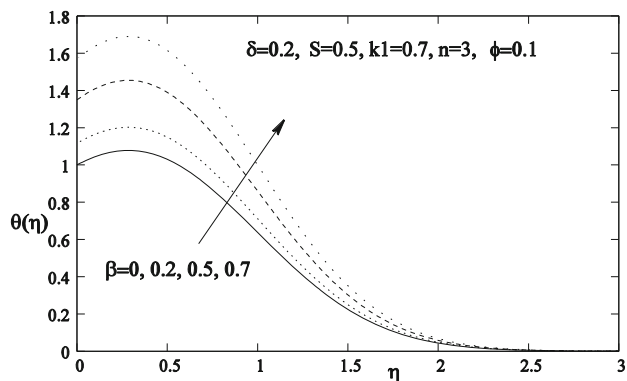


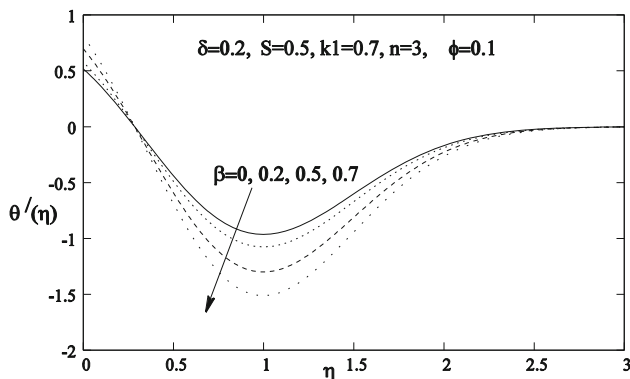
Figure 5. (a) Velocity profiles for different values of velocity slip parameter, (b) shear stress profiles for different values of velocity slip parameter and (c) temperature profiles for different values of velocity slip parameter for nanoparticles of different shapes.

intensifies. Shear stress reduces with the rising values of δ (figure 5b). Temperature decreases in this case (figure 5c). Higher temperature is noted for higher values of n . Temperature overshoot is noted near the plate (figure 5c).

Due to thermal slip, temperature increases rapidly near the plate since a modest quantity of heat is transferred from the fluid to the plate, but away from the plate, the increase in temperature is comparatively less. Temperature overshoot is observed near the plate



(a)



(b)

Figure 6. (a) Temperature profiles for different values of thermal slip parameter and (b) temperature gradient profiles for different values of thermal slip parameter.

(figure 6a), i.e., from the fluid, heat is transported to the plate. Temperature gradient profiles for various values of the thermal slip parameter can be found in figure 6b.

5. Concluding remarks

Forced convection flow of Cu–water nanofluid with randomly formed nanoparticles in the presence of slip over a permeable plate has been studied. Some interesting observations are listed as follows:

- (i) The fluid velocity is found to increase with increasing values of the nanoparticle volume fraction parameter, suction parameter, permeability parameter of the porous medium and the slip parameter corresponding to velocity. However, the temperature decreases with all those physical parameters.
- (ii) The fluid temperature increases with the increase in thermal slip parameter.

- (iii) The thermal boundary layer thickness increases with increasing values of n .
- (iv) The temperature overshoot near the plate is noted for higher values of the volume fraction of nanoparticles.
- (v) The shear stress reduces with a rise in the permeability parameter and the rising values of the slip parameter corresponding to velocity.

Acknowledgements

The authors thankfully acknowledge the help and support received from the learned reviewers and editors for their constructive suggestions, which improved the quality of the paper. Also, the authors thank Prof. M Taylor for reading the paper.

References

- [1] S U S Choi, in: *The Proceedings of the ASME International Mechanical Engineering Congress and Exposition* (San Francisco, USA, ASME, FED, 231/MD) **66**, 99–105 (1995)
- [2] J Buongiorno, *J. Heat Transf.* **128**, 240 (2006)
- [3] R K Tiwari and M K Das, *Int. J. Heat Mass Transf.* **50**, 2002 (2007)
- [4] M Mustafa, T Hayat, I Pop, S Asghar and S Obaidat, *Int. J. Heat Mass Transf.* **54**, 5588 (2011)
- [5] S Nadeem and C Lee, *Nanoscale Resc. Lett.* **7(94)**, 1 (2012)
- [6] S Nadeem, R Ul Haq and Z H Khan, *Alex. Engng. J.* **53**, 219 (2014)
- [7] ST Hussain, S Nadeem and R Ul Haq, *Eur. Phys. J. Plus* **129**, 161 (2014)
- [8] K Das, P R Duari and P K Kundu, *Alex. Eng. J.* **53**, 737 (2014)
- [9] F Mabood, W A Khan and A I M Ismail, *J. Magn. Magn. Mater.* **374**, 569 (2015)
- [10] T Hayat, A Aziz, T Muhammad and A Alsaedi, *Chin. J. Phys.* **55**, 1495 (2017)
- [11] E H Hafidzuddin, R Nazar, N M Arifin and I Pop, *Eur. J. Mech. B Fluids* **65**, 515 (2017)
- [12] C Choi and C Kim, *Phys. Rev. Lett.* **96**, 066001(2006)
- [13] T Hayat, T Javed and Z Abbas, *Int. J. Heat Mass Transf.* **51**, 4528 (2008)
- [14] S Mukhopadhyay, K Bhattacharyya and G C Layek, *Int. J. Heat Mass Transf.* **54(13–14)**, 2751 (2011)
- [15] M Sajid, Z Abbas, N Ali, T Javed and I Ahmad, *Walailak J. Sci. Technol.* **11**, 1093 (2014)
- [16] A K Verma, A K Gautam, K Bhattacharyya, A Banerjee and A J Chamkha, *Pramana – J. Phys.* **95**, 173 (2021)

- [17] A K Gautam, A K Verma, K Bhattacharyya, S Mukhopadhyay and A J Chamkha, *Waves Random Complex Media*, <https://doi.org/10.1080/17455030.2021.1979274> (2021)
- [18] A Banerjee, K Bhattacharyya, S K Mahato and A J Chamkha, *Chin. Phys. B* **31(4)**, 044701 (2022)
- [19] S Mukhopadhyay and G C Layek, *Meccanica* **44**, 587 (2009)
- [20] S Mukhopadhyay, P R De, K Bhattacharyya and G C Layek, *Meccanica* **47**, 153 (2012)
- [21] A Aziz, W A Khan and I Pop, *Int. J. Therm. Sci.* **56**, 48 (2012)
- [22] J V Ramana Reddy, V Sugunamma, N Sandeep and C Sulochana, *J. Nigerian Math. Soc.* **35**, 48 (2016)
- [23] T Chakraborty, K Das and P K Kundu, *J. Mech. Sci. Technol.* **31(5)**, 2443 (2017)
- [24] R L Hamilton and O K Crosser, *J. Ind. Eng. Chem. Fund.* **1**, 187 (1962)
- [25] K Das, *J. Mech. Sci. Technol.* **28(12)**, 5089 (2014)
- [26] H Blasius, *Z. Math. Phys.* **56**, 1 (1908)
- [27] L Howarth, *Proc. R. Soc. Lond. A* **164**, 547 (1938)
- [28] R Cortell, *Appl. Math. Comput.* **170**, 706 (2005)
- [29] A Ishak, R Nazar and I Pop, *Int. J. Heat Mass Transf.* **50**, 4743 (2007)